Human Cell
https://doi.org/10.1007/s13577-023-00978-4

CELL LINE

Generation of an induced pluripotent stem cell line from a patient with epileptic encephalopathy caused by the CYFIP2 R87C variant

Isabelle Leticia Zaboroski Silva[1] · Rubens Gomes-Júnior[1] · Evelin Brandão da Silva[1] · Isadora May Vaz[2] · Valderez Ravaglio Jamur[2] · Bruno Solano de Freitas Souza[3,4] · Patrícia Shigunov[1]

Received: 15 May 2023 / Accepted: 21 August 2023
© The Author(s) under exclusive licence to Japan Human Cell Society 2023

Abstract

Induced pluripotent stem cells (iPSCs) opened the possibility to use patient cells as a model for several diseases. iPSCs can be reprogrammed from somatic cells collected in a non-invasive way, and then differentiated into any other cell type, while maintaining the donor´s genetic background. CYFIP2 variants were associated with the onset of an early form of epileptic encephalopathy. Studies with patients showed that the R87C variant seems to be one of the variants that causes more severe disease, however, to date there are no studies with a human cell model that allows investigation of the neuronal phenotype of the R87C variant. Here, we generated an iPSC line from a patient with epileptic encephalopathy caused by the CYFIP2 R87C variant. We obtained iPSC clones by reprogramming urinary progenitor cells from a female patient. The generated iPSC line presented a pluripotent stem cell morphology, normal karyotype, expressed pluripotency markers and could be differentiated into the three germ layers. In further studies, this cell line could be used as model for epileptic encephalopathy disease and drug screening studies.

✉ Patrícia Shigunov
patricia.shigunov@fiocruz.br

[1] Stem Cell Basic Biology Laboratory, Instituto Carlos Chagas, Fiocruz PR, Curitiba, PR 81310-020, Brazil

[2] Core for Cell Technology, School of Medicine, Pontifícia Universidade Católica do Paraná, Curitiba, PR 80215-901, Brazil

[3] Gonçalo Moniz Institute, Oswaldo Cruz Foundation (FIOCRUZ), Salvador 40296-710, Brazil

[4] D'Or Institute for Research and Education (IDOR), Salvador 41253-190, Brazil

Published online: 30 August 2023

Graphical abstract

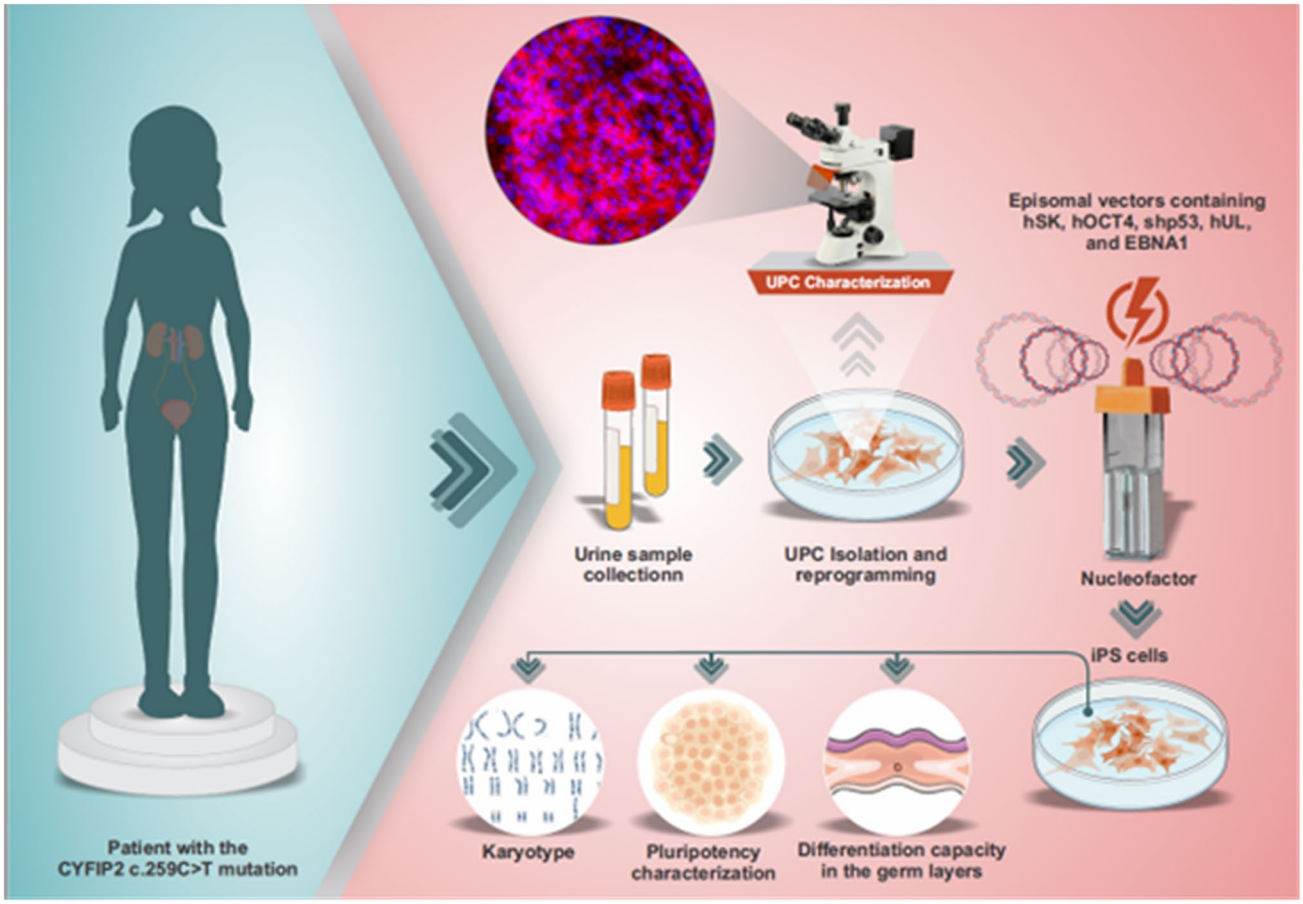

Keywords iPSC · CYFIP2 variant · Epileptic encephalopathy

Introduction

Since Yamanaka's first description [1], induced pluripotent stem cells (iPSC) are being used as models for different types of diseases (reviewed in [2]). These cells are generated by reprogramming patients' somatic cells, obtained from different sources. The resulting iPSCs present the hallmarks of pluripotency, including self-renewal and the ability to differentiate in any cell type derived from the three germ layers. This technology made possible to obtain differentiated cells that usually would be difficult to access in patients, such as neurons and cardiomyocytes, maintaining the genetic background that could be related to the diseases [2]. These characteristics make iPSCs an unique opportunity to develop relevant patient-derived cell models for disease modeling, such as molecular studies and drug screening [2].

Epileptic encephalopathy (E.E.) is a neural disorder that causes muscle spasms, hypsarrhythmia, and intellectual disability [3]. Variants in different genes have been associated with this disease, including variants in the CYFIP2 gene [4]. CYFIP2 is a protein that participated in the WAVE regulatory complex, involved in the branched actin filaments polymerization, a critical process during neuronal development [5–7]. In addition, CYFIP2 can interact with FMRP, an RNA-binding protein that takes part in post-transcriptional regulation in neurons [8], placing CYFIP2 in the context of mRNA regulation. Among the CYFIP2 variants associated with E.E. development, the R87C variant is described as the one that causes more severity of symptoms [9]. This variant is a substitution of arginine for cysteine in position 87 of the protein, caused by a single nucleotide substitution in exon 4 of the gene (c.259 C>T; p. Arg87Cys) [4]. Studies with animal models showed that CYFIP2 is expressed exclusively in neurons [10] and enriched in excitatory synapses [11]. A recent study described an animal model for the R87C variant, which showed that Cyfip2$^{+/R87C}$ mice could manifest a similar phenotype to the human neurodevelopmental disorder [12]. Although this study has found a decrease in

CYFIP2 protein levels, the presence of gliosis, and the differential expression of genes involved in post-transcriptional regulation in the Cyfip2$^{+/R87C}$ mice brains, there is still a lack of understanding about the effect of molecular mechanisms and neuronal phenotype caused by the R87C variant in humans.

Here, we establish an iPSC R87C line derived from an E.E. patient. The iPSC R87C C8 line presented the features of a pluripotent stem cell, such as morphology, expression of pluripotency markers, and capacity to differentiate into the three germ layers. The cell line established here could contribute to understanding the molecular impact of the R87C variant and be used as a model for drug screening aiming at the patients' treatment.

Materials and methods

Patient recruitment and ethics committee

The project was approved by the Research Ethics Committee (CEP) of Fiocruz, and by the National Research Ethics Committee (CONEP), under opinion number 3.856.868, CAAE: 16918819.7.0000.5248. The patient is a 3-year-old female diagnosed with epileptic encephalopathy and with the c.259C>T (p.Arg87Cys) mutation in the CYFIP2 gene identified by exome sequencing examination. The collection and subsequent processing of the patient's sample were authorized by her parents via an Informed Consent Form (ICF).

Isolation of urinary progenitor cells

Urinary progenitor cells (UPC) were obtained from the patient´s urine samples following a protocol, adapted from Steichen et al. and Zhou et al. [13, 14]. For UPC isolation, urine was collected from the patient using a collection bag. About 10 ml of urine from the patient and 40 ml of urine from the family were used for the procedure. The samples were centrifuged at 400×*g* for 5 min, the supernatant was discarded, the cell pellet was washed with 40 ml of washing buffer (PBS 1× 1% streptomycin/penicillin 0.25 g amphotericin B), and the samples were centrifuged again at 400×*g* for 5 min. The supernatant was gently removed, and the pellet was resuspended with UPC medium (50% DMEM, 10% SFB, 1% penicillin/streptomycin, 1% non-essential amino acids and 50% REBM medium (Lonza) supplemented with REGM factors (Lonza) supplemented with 5 ng/ml bFGF. The cell solution from each sample was plated into a 24-well plate well pre-coated with 0.1% gelatin solution (Sigma). UPC colony formation was monitored for 10 days, and after reaching 80–90% confluence, the cells were expanded into two wells of a 12-well plate, and after reaching confluence again, expanded into eight wells of a 12-well plate. From then on, the cells were frozen or proceeded to the reprogramming step.

Reprogramming of urinary progenitor cells and iPSC cultivation

To obtain iPSCs from the patient's UPC, the reprogramming protocol was adapted from Steichen et al. and Zhou et al. [13, 14]. For reprogramming the patient's UPC (UPC CYFIP2 R87C), UPC cells from two wells of the 12-well plate were used. The cells were grown in the UPC medium containing 2 µM thiazovivin (ROCK inhibitor) 3 h before electroporation. Nucleofector 2B in program W-001 and 4 µg of the following plasmids containing reprogramming factors were used for electroporation: pCXLE-hSK, pCXLE-hOCT3/4-shp53-F, pCXLE-hUL and pCXWB-EBNA1 (Addgene #27077, #27078, #27080 and #41857). After electroporation, cells were cultured in 5 ng/ml bFGF UPC medium in six-well plate wells pre-coated with Matrigel (Corning). The next day (D1), the medium was changed to UPC 5 ng/ml bFGF medium. Two days later (D3), the medium was changed to 50% UPC 5 ng/ml bFGF medium and 50% StemFlex (Gibco). From the following medium change (D5), the medium used was StemFlex which was changed every other day. The cells were cultivated until the appearance of colonies with morphological characteristics of pluripotent stem cells, such as rounded cells, with a high nucleus/cytoplasm ratio, and rounded colonies with defined borders. Then, these colonies were manually selected to expand into wells of a 24-well plate coated with Matrigel and were referred to as clones. Clones that survived selection were expanded and cryopreserved.

To select the iPSC clones to be characterized, the cells were thawed in a six-well plate pre-coated with Matrigel (Corning) in StemFlex medium (Gibco) with 2 µM of thiazovivin (Sigma). Clones that kept pluripotent stem cell morphology were carried to karyotype analysis. Then, clones were expanded in pre-coated wells with Matrigel (Corning) in StemFlex medium (Gibco), for RNA extraction, and plated using Accutase™ (Stem Cell Technologies) for immunofluorescence and differentiation assays.

Karyotype of the iPSC clones

To exclude the possibility of chromosomal aberrations, a karyotype assay was performed in iPSC clones as previously described [15]. For chromosome analysis, cells were treated with colchicine to stop them in the metaphase phase of the cell cycle. Next, they were submitted to a hypotonic solution with potassium chloride for 10 min at 37 °C and then incubated for 10 min at − 20 °C with Carnoy's fixative solution, a mixture of methanol and acetic

acid. First, with the fixative solution at a 3:1 proportion, then two times at a 2:1 proportion. Lastly, cells were submitted to the karyotyping using the G-banding technique.

Differentiation assays

To characterize the generated iPSC pluripotency competence, the cells were induced for differentiation in the three germ layers. For endodermal differentiation, 1×10^5 cells/well were plated in a 24-well plate pre-coated with Matrigel (Corning) in StemFlex medium (Gibco) with 2 µM of thiazovivin (Sigma). After 24 h, the medium was changed to remove the ROCK inhibitor. On the following day (D0), cells were endodermally induced by adding 3 µM of CHIR99021 and 50 ng/ml of Activin A to the basal medium (RPMI 1% L-glutamine, 1% non-essential amino acids, 1× B-27 minus insulin) during the medium replacement. After 2 days (D2), the medium was changed to the base medium containing 50 ng/ml Activin A. On D4, cells were fixed for immunofluorescence assay or had RNA extracted.

For mesodermal differentiation, 2.5×10^5 cells/well were plated in a 24-well plate pre-coated with Matrigel (Corning) in mTeSR Plus medium (Stem Cell Technologies) with 10 µM of Y-27632 (ROCK inhibitor, Sigma). After 24 h, the medium was changed to remove the ROCK inhibitor, and on the next day, cells had the medium changed one more time to reach maximum confluency. On D0, cells were mesodermally induced by adding 12 µM of CHIR99021 to the base medium (RPMI 1× B-27 minus insulin) during the medium replacement. On D1, cells were fixed for immunofluorescence assay or had RNA extracted.

For ectodermal differentiation, 2.5×10^5 cells/well were plated in a six-well plate pre-coated with Matrigel (Corning) in StemFlex medium (Gibco) with 2 µM of thiazovivin (Sigma). The next day (D0), the medium was changed to Neural Induction Medium (Neurobasal Medium 1× Neural Induction Supplement, Thermo Fisher Scientific). Following the manufacturer, the medium was changed on days 3, 5, and 7 (D5 and D7 with double the medium). On D8, cells were fixed for immunofluorescence assay or had RNA extracted.

The differentiation of SP1C8 cells into cortical neurons was based on a previous described protocol by Ahn et al. (2021) [16]. The SP1C8-derived neural progenitor cells were plated onto poly-L-ornithine/laminin (Sigma) and cultured in Neural Media [DMEM/12 (Gibco), 0.5 × N2 Supplement (GeminiBio), 0.5 × B27 Supplement (Gibco), 1% Penicillin/Streptomycin (Gibco), 20 ng/ml BDNF (Gibco), 20 ng/ml GDNF (Gibco)], and 5 µM thiazovivin (Sigma). After 14 days, the cells were re-plated using Stem Pro Accutase (Gibco) and maintained for another 14 days, until day 28, when the cells were fixed to staining.

Immunofluorescence

For the marker's expression analysis at protein levels, immunofluorescence of UPC, pluripotency, and germ layers markers was conducted. For immunofluorescence of epithelial, renal epithelial, and fibroblast markers, UPC and NHDF were fixed with 4% PFA, permeabilized with PBS 1× 0.5% Triton X-100, blocked with 5% PBS/BSA, incubated with anti-E-cadherin, anti-β-catenin, anti-CD13, anti-Fibronectin, or anti-Vimentin, and incubated with goat anti-mouse 546-conjugated or goat anti-Rabbit 546-conjugated secondary antibody (information about the antibodies are detailed in Table S1). Visualization was performed on a deconvolution microscope. The photos in this report were treated in PhotoGIMP software (version 2.10.20) to improve brightness and contrast and to make the images superimposed (Merged).

For immunofluorescence of pluripotency markers, iPSCs were fixed with 4% PFA, permeabilized with PBS 1× 0.5% Triton X-100, blocked with 5% PBS/BSA, incubated with anti-OCT4 antibody, anti-TRA-1-60, anti-TRA-1-81, anti-SSEA3, or anti-SSEA4, and incubated with rabbit anti-Goat 594-conjugated or donkey anti-Mouse 488-conjugated secondary antibody. Visualization was performed on a deconvolution microscope. The photos in this report were treated in PhotoGIMP software (version 2.10.20) to improve brightness and contrast and to make the images superimposed (Merged).

For immunofluorescence of germ layers markers, cells were fixed with 4% PFA, permeabilized with PBS 1× 0.5% Triton X-100, blocked with 5% PBS/BSA, incubated with anti-HNF4a antibody (endodermal marker), anti-Brachyury (mesodermal marker), anti-Nestin (ectodermal marker) or anti-PAX6 (ectodermal marker), and incubated with donkey anti-Mouse 488-conjugated or goat anti-Rabbit 546-conjugated secondary antibodies. Visualization was performed on a deconvolution microscope. The photos in this report were treated in PhotoGIMP software (version 2.10.20) to improve brightness and contrast and to make the images superimposed (Merged).

In order to evaluate the expression of immature neurons marker, the SP1C8-derived cortical neurons were fixed with 4% PFA, permeabilized with PBS 1× 0.5% Triton x-100, blocked with 5% PBS/BSA, incubated with anti-TUJ1, and incubated with anti-Rabbit 488-conjugated secondary antibody. Analyzes were performed using Operetta CLS High-Content Imaging System and image acquisition by Harmony 4.8 software (PerkinElmer).

RNA extraction and reverse transcription

For the markers expression analysis at mRNA levels, RNA extraction was performed with the RNeasy kit (Qiagen),

according to the manufacturer's instructions. Briefly, cells were counted and lysed with lysis buffer, and RNAse-free 70% ethanol was added. The solution was added to a column, the sample was treated with DNAse, washed a few times with wash buffer, and the RNA was eluted in 30 µl of RNAse-free ultrapure water. RNA was quantified using NanoDrop One (Thermo Fisher Scientific) and stored at − 80 °C. A reverse transcription reaction was carried on to obtain the complementary DNA (cDNA), and the RT Improm-II enzyme (Promega) was used, according to the manufacturer's instructions. Briefly, 1 µg of RNA was incubated with oligoDT primers and then incubated in the buffer containing the reverse transcriptase enzyme, nucleotides (dNTP), and RNAse inhibitor. At the end of the process, the cDNA was diluted in 100 µl of ultrapure water and stored at − 20 °C.

Polymerase chain reaction (PCR)

To perform the analysis of the expression of pluripotency and germ layer markers by quantitative PCR (qPCR), the GoTaq® qPCR Master Mix reagent (Promega) was used, with the primers of pluripotency and germ layers markers, and the normalizing gene GAPDH (Table S2). The reaction of 10 µl, in technical triplicate, was performed in the real-time PCR platform of the Carlos Chagas Institute, in the LightCycler® 96 equipment (Roche Life Sciences) or QuantStudio5 (Thermo Fisher Scientific), and the results were analyzed in the software of the same manufacturer. Expression analysis was performed using fold to GAPDH, and the result was analyzed by Student's *t*-test, and a $p \leq 0.05$ was considered significant in GraphPad Prism software (version 7.05).

Sequencing of CYFIP2 gene

To confirm the presence of the variant in the iPSC clones, exon 4 of the CYFIP2 was sequenced. Cells were resuspended in TES buffer (10 mM Tris HCl 1 M pH 8.0, 50 mM EDTA 0.5 M pH 8.0, 0.5% SDS) with proteinase K and incubated at 55 °C overnight. Then, potassium acetate (concentration 3 M) was added, the sample was incubated at 20 °C for 10 min, and centrifuged. The supernatant was recovered, and isopropanol was added to precipitate the DNA molecule. After centrifugation, the DNA pellet was resuspended in ultrapure water. PCR was performed using CYFIP2 primers to obtain the fragment of exon 4 (Table S2). Then, the PCR product was sent to GoGenetic (Curitiba, PR, Brazil) to be sequenced.

DNA separation by capillary electrophoresis

Approximately 2 ng of the extract was added to the PCR amplification mix and amplified using the Applied Biosystem 2720 Thermo Cycler. Tandem repeat analysis of 23 STR loci using the PowerPlex® Fusion System (Promega) was performed. Amplified products were separated on an Applied Biosystems®3130xl Genetic Analyzer. Fragment analysis was performed using the GeneMapper® software 5. The size of each fragment of amplified DNA was determined by comparison to the internal lane standard (WEN 500) provided by the manufacturer. The representation of the STR loci DYS391 was not shown, because it had no amplification peak.

Results

Urinary progenitor cells (UPC) were isolated from the patient's urine according to with previously described [13] and further characterized (Fig. 1). The cell morphology assembled to type II UPC (Fig. 1A). The cells expressed the renal epithelial markers L1CAM and SCL2A1 and did not express the fibroblast marker TWIST1 at the mRNA level (Fig. 1B). Compared to the NHDF fibroblast lineage, the isolated UPC has an increased expression of the epithelial markers β-catenin and E-cadherin and the renal epithelial marker CD13, while the expression of the fibroblast markers Fibronectin and Vimentin were decreased, at proteins levels (Fig. 1C; Fig. S1). The isolated UPC also expressed pluripotency markers TRA-160, TRA-1-81, SSEA3, and SSEA4, but not OCT4 (Fig. 1D; Figs. S2–S5).

To generate iPSC clones, UPC in passage 3 was electroporated with episomal expression vectors containing Yamanaka's factors. The clones that presented round colonies were picked up manually, expanded, and cryopreserved. We obtained 22 clones that were frozen. For a first screening, 6 clones were stained for OCT4, TRA-1-60, and TRA1-81 (data not shown), and 2 were randomly chosen for further characterization (clones SP1C8 and SP1C17). Clone SP1C17 showed all the pluripotency markers expression and was able to differentiate into endoderm and mesoderm, but not to ectoderm even after several attempts (data not shown), so we kept working with the clone SP1C8. Clone SP1C8 (iPSC R87C C8) grew in round colonies after thawing up to 27 passages (Fig. 2A) and showed chromosomal stability determined by G-band karyotyping (Fig. 2B), proceeding to further analysis. The expression of pluripotency markers was analyzed by immunostaining and qPCR. iPSC R87C C8 showed expression of OCT3/4, NANOG, and REX1 at RNA levels (Fig. 2D; Fig. S2) and OCT3/4, TRA-1-60, TRA-1-81, SSEA4, and SSEA3 at protein levels (Fig. 2C; Figs. S3–S6). Sequencing analysis showed the presence of heterozygosity in exon 4 of the CYFIP2 gene (Fig. 2E), confirming the presence of the R87C variant. PCR analysis of total DNA extraction showed no presence of EBNA1 (Fig. 2F), confirming the loss of the episomal vectors.

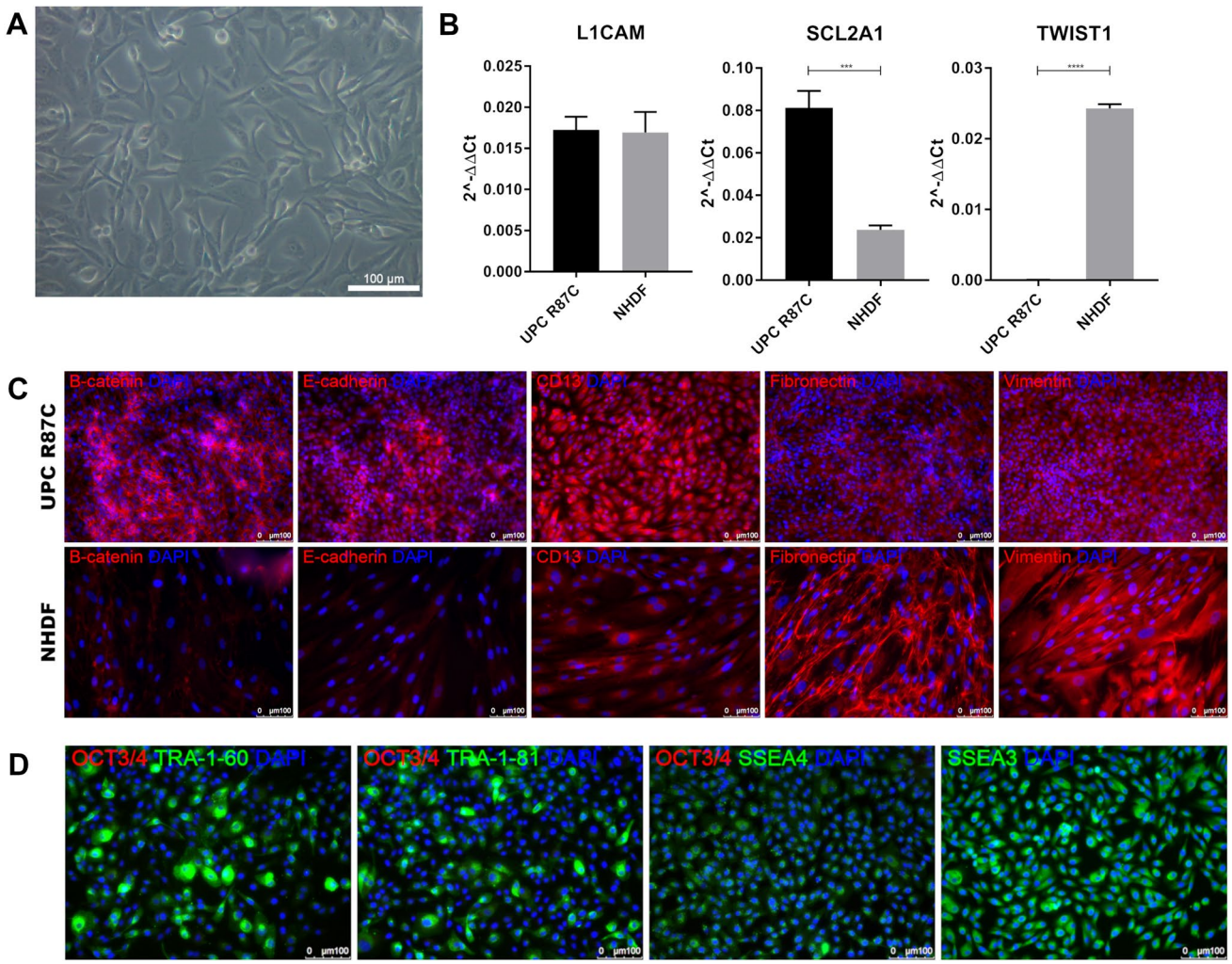

Fig. 1 Isolation and characterization of urinary progenitor cells (UPC). **A** Representative phase-contrast image of the isolated UPC in gelatin coating, in high confluency at passage 2. Scale bar: 100 µm. **B** mRNA expression of renal epithelial markers L1CAM and SCL2A1 and fibroblast marker TWIST1 in UPC R87C (black) and fibroblast lineage NHDF (grey). Expression levels are normalized by GAPDH mRNA levels. **C** Immunofluorescence images of epithelial, renal epithelial, and fibroblast markers expression in UPC and NHDF. β-catenin, E-cadherin, CD13, Fibronectin, or Vimentin: red. DAPI: blue. Scale bar: 100 µm. **D** Immunofluorescence images of pluripotency markers expression in UPC. OCT3/4: red. TRA-1-60, TRA-1-81, SSEA4 or SSEA3: green. DAPI: blue. Scale bar: 100 µm

The capacity to differentiate into three germ layers was analyzed by inducing the cells to endoderm, mesoderm, and ectoderm. iPSC R87C C8 was able to differentiate into endoderm (HNF4a), primitive mesoderm (BRACH), and neural progenitor cells (PAX6) (Fig. 3A; Fig. S7). Additionally, the expression of CXCR4, SOX17 (endoderm), TBTX, EOMES (mesoderm), PAX6, and NEUROD1 (ectoderm) markers was accessed by qPCR (Fig. 3B; Fig. S8). The genetic identity by fingerprinting was performed by STR analysis (available with the authors). Finally, the test for *Mycoplasma* sp. showed negative results (data not shown). Cortical neurons derived from the iPSC SP1C8 showed positive staining for TUJ1, an immature neuron marker, and showed neurites formation (Fig. 3C), indicating the neuronal differentiation capacity.

Discussion

Since the description of the involvement of CYFIP2 with the onset of E.E., many studies were performed to understand the molecular mechanisms of the CYFIP2 variants and to establish the best models to be used for it. Overexpression of the CYFIP2 variants in HEK and HeLa cell lines was first used to attempt to understand the cellular phenotype. The data showed that the R87 variants could lead to a disorganization of the actin filaments, favor the formation of cellular aggregates, and impair the formation of stress granules [4, 17], but how these could generate the patients' phenotype was still unclear. Meanwhile, Begeman and collaborators isolated fibroblasts from patients with E.E. and observed that CYFIP2 variants may impair dorsal ruffle formation,

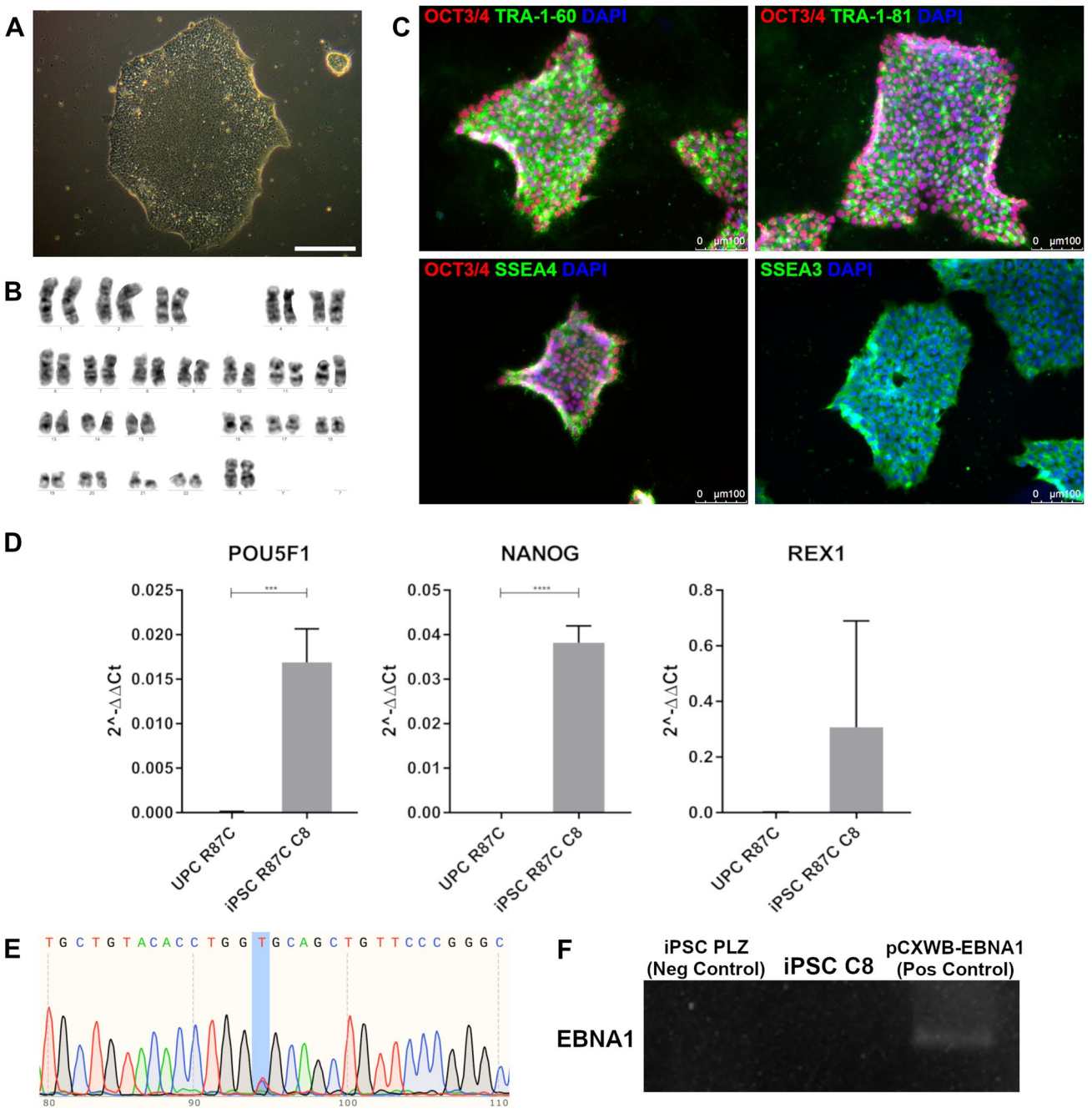

Fig. 2 Characterization of iPSC R87C C8 as its pluripotency. **A** Bright-field image of an iPSC R87C C8 colony on Matrigel coating, in passage 13. Scale bar: 100 µm. **B** Karyogram of iPSC R87C C8 by G-banding technique, showing no chromosomal abnormalities (46, XX [20]). **C** Immunofluorescence images of pluripotency markers expression in iPSC R87C C8. OCT3/4: red. TRA-1-60, TRA-1-81, SSEA4 or SSEA3: green. DAPI: blue. Scale bar: 100 µm. **D** mRNA expression of pluripotency markers OCT4(POU5F1), NANOG, and REX1 in UPC R87C (black) and iPSC R87C C8 (grey). Expression levels are normalized by GAPDH mRNA levels. **E** Sequencing of exon 4 of CYFIP2 gene in iPSC R87C C8, showing the heterozygous mutation (highlighted in blue). **F** PCR of EBNA1 from total DNA. iPSC PLZ (Neg Control): reaction negative control for another well-established hPSC showing no EBNA1 expression. pCXWB-EBNA1 (Pos Control): reaction positive control plasmid containing the EBNA1 gene

a structure involved in cellular migration, but not affect the migration capacity of these cells [9]. The authors justified that the low CYFIP2 expression in the fibroblast could be the reason for the results obtained, as CYFIP2 expression is usually expressed in higher levels in the central nervous system. Regarding animal models, Cyfip2 knockout leads to early postnatal lethality and changes in mRNA content in mice brains [18], and lower expression of Cyfip2 leads to

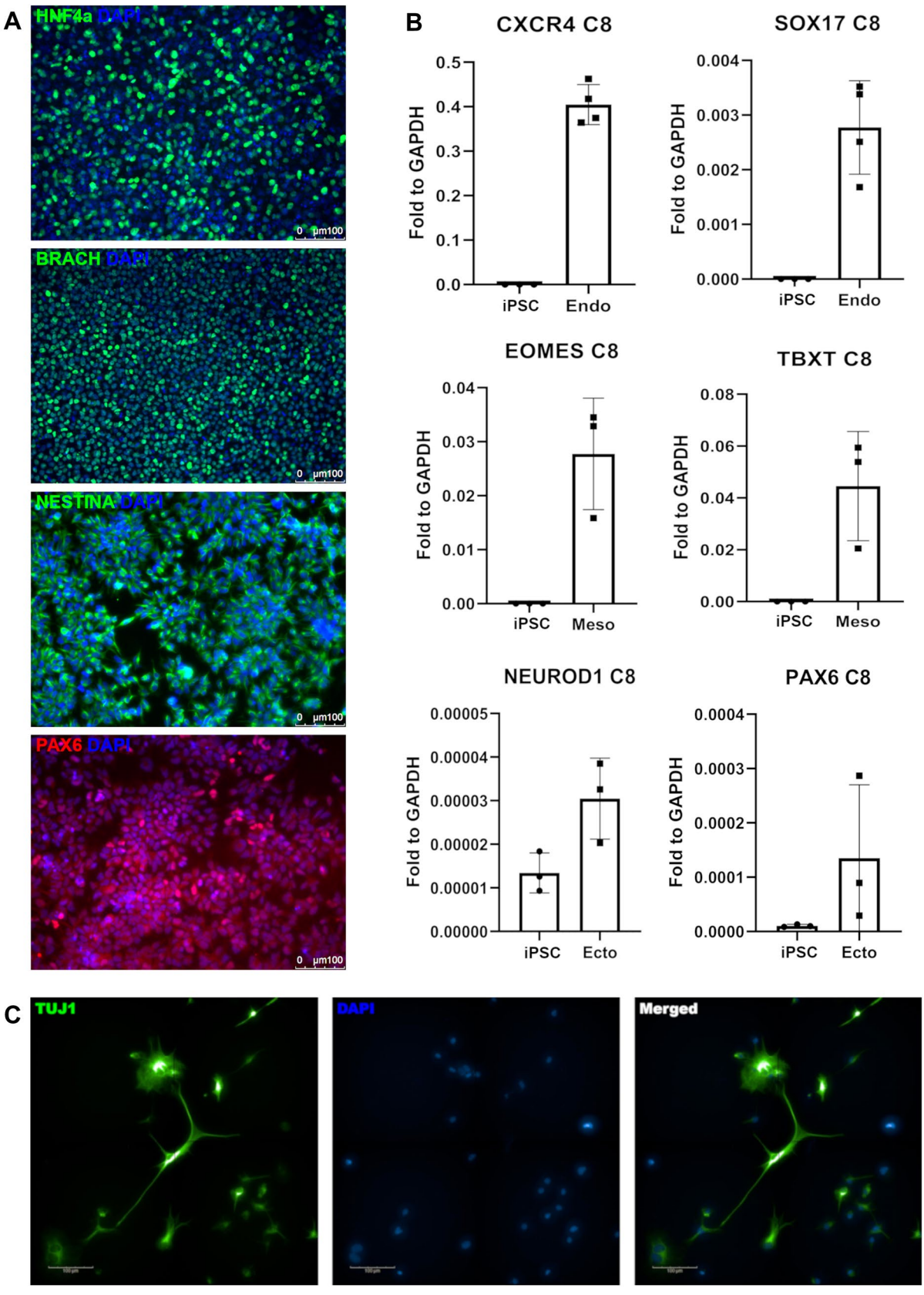
A
HNF4a DAPI
BRACH DAPI
NESTINA DAPI
PAX6 DAPI
0 µm100
B
CXCR4 C8
SOX17 C8
EOMES C8
TBXT C8
NEUROD1 C8
PAX6 C8
Fold to GAPDH
iPSC
Endo
Meso
Ecto
C
TUJ1
DAPI
Merged

◂**Fig. 3** Differentiation of iPSC R87C C8 in the three germ layers. **A** Immunofluorescence images of endoderm (HNF4a: green), mesoderm (BRACHYURI: green), and ectoderm (PAX6: red; Nestin: green) markers after induced differentiation of iPSC R87C C8 for each germ layer. DAPI: blue. Scale bar: 100 µm. **B** mRNA expression of endoderm (CXCR4, SOX17), mesoderm (BRACH/TBXT, EOMES), and ectoderm (PAX6, NEUROD1) markers before and after induced differentiation of iPSC R87C C8 for each germ layer. Expression levels are normalized by GAPDH mRNA levels. **C** Immunofluorescence images of SP1C8-derived cortical neurons stained for TUJ1 (green). DAPI: blue. Scale bar: 100 µm

excitatory/inhibitory imbalance in the brain of these animals [19]. Although these knockdown and knockout animals point to a better comprehension of the CYFIP2 role, they may not be the best model to analyze the impact of CYFIP2 variants on E.E. A study described a CYFIP2 R87C mice model which resembles the symptoms presented in human E.E., like microencephaly and seizure susceptibility [12]. The authors also showed that the R87C mice presented gliosis and layer disorganization of mice brains. Despite the interesting results obtained using the animal model, for more detailed information, the authors used overexpression of the CYFIP2 variant in HEK293T cells, which did not resume the genotype presented by the patients. That is the main reason for the development of a cellular model, as we proposed in this present study, that should be used complementary to animal models to better understand the molecular impact of the CYFIP2 R87C variant and to be a starting point for drug screening assays.

Regarding the neurogenic capacity, we could see that the iPSC C8 was able to differentiate into cortical neurons, indicating that the hiPSC established in this study can be used to investigate the role of R87C variant and its impact in neurodevelopment. Preliminary, in the neural progenitor cells derived from the iPSC C8, we observed that the PAX6 levels are very similar between the two cell lines and NEUROD1 seems to have differences. Due to the low expression of NEUROD1 for both lines, these observed variations may be the result of reduced sensitivity of the equipment in the final cycles of qPCR. Furthermore, the lineage is unique, preventing the performance of statistical analyzes that could determine the significance of these variations. Furthermore, the impact of the R87C variant on NEUROD1 expression is not known. If this will affect the neurogenic ability of the cells is an interesting point to be explored in the next steps.

The UPCs were isolated and characterized accordingly to the literature [14, 20]. The UPC are cells derived from the renal epithelial tissue that should express epithelial and renal epithelial markers and could express some fibroblast markers at a lower level [20]. However, some studies showed that UPC also expresses pluripotent and mesenchymal stem cell markers and even could be differentiated in different cell lines [21–23]. Indeed, we found that the UPC isolated from our patient expressed some pluripotent markers at protein levels. Interestingly, one of the isoforms of POU5F1 (OCT4) is described as present in renal tissue and could be found in cells derived from it [24]. We were not able to see an expression of OCT4 at mRNA and protein levels. For the qPCR assay, we designed primers that were specifically for the OCT4 isoform A, which is described as a pluripotent marker [25]. We could not say the specificity of the antibody used in the immunofluorescence assay, but it seems to be specific for the pluripotent isoform. We did not conduct differentiation assays using our isolated UPC, as the study's goal was reprogramming these cells. Unlike UPC, iPSCs can be expanded multiple times without reaching senescence [23], removing the need for multiple collections. Also, because of the auto renovation capacity, iPSCs could be genetically modified to obtain isogenic controls, which is interesting in understanding rare diseases. Finally, using iPSCs in neurodevelopmental disorders allows observation of the phenotype from the pluripotent state, which helps determine at which stage genetic variants begin to impact development.

Conclusions

Here, we successfully established an iPSC model of the CYFIP2 R87C variant. The iPSC presented all the features of a pluripotent stem cell, such as pluripotent markers expression and three germ layers differentiation capacity. Also, the cell line did not present chromosomal abnormalities and could be safely used in further studies about the molecular impact of the CYFIP2 R87C variant in the neurodevelopment of E.E. in vitro and could be used as a starting point for drug screening studies to find drugs that act directly on the mutated CYFIP2, favoring the specificity of the medication and improving the quality of life for patients.

Supplementary Information The online version contains supplementary material available at https://doi.org/10.1007/s13577-023-00978-4.

Acknowledgements The authors thank Dra Anny Robert and Dra Bruna Marcon of the Platform of Microscopy of Fiocruz PR for their help in image acquisition and training. We also thank MSc Crisciele Kuligovski of Cell Culture Lab for the mycoplasma testing. Lastly, we thank Wagner Nagib for the abstract graphical design.

Author contributions ILZS designed and conducted most of the experimental work and was a major contributor to writing the manuscript. RG-J and EBS conducted experimental work. IMV and VRJ conducted the karyotyping acquisition and analysis. BSFS contributed to STR acquisition and analysis. PS contributed to study conception, supervision, and project administration.

Funding This research was funded by Conselho Nacional de Desenvolvimento Científico e Tecnológico—CNPq/Instituto Carlos Chagas No. 15/2019—PROEP/ICC—442324/2019-7. PS received a scholarship from Conselho Nacional de Desenvolvimento Científico e Tecnológico—CNPq. The funders had no role in the study design, data

collection and analysis, decision to publish, or preparation of the manuscript.

Data availability Table S1: Antibodies details; Table S2: Primers list; Figure S1: Expression of epithelial, renal epithelial, and fibroblast markers in UPC and NHDF; Figure S2: Expression of POU5F1 (OCT4), NANOG, and REX1 in ESC H1, iPSC R87C C8, and UPC. Figure S3: Expression of OCT4 and SSEA4 in ESC H1, iPSC R87C C8, and UPC. Figure S4: Expression of OCT4 and TRA-1-60 in ESC H1, iPSC R87C C8, and UPC. Figure S5: Expression of OCT4 and TRA-1-81 in ESC H1, iPSC R87C C8, and UPC. Figure S6: Expression of SSEA3 in ESC H1, iPSC R87C C8, and UPC. Figure S7: Expression of germ layers' markers in differentiated iPSC R87C C8. Figure S8: Expression of germ layers markers on ESC H1 and iPSC R87C C8 differentiation.

Declarations

Conflict of interest The authors declare that they have no conflict of interest.

Ethical approval The study has approval by the Research Ethics Committee (CEP) of Fiocruz, and by the Brazilian National Research Ethics Committee (CONEP), under opinion number 3.856.868, CAAE: 16918819.7.0000.5248.

Consent to participate All study participants provided written informed consent prior to enrolment.

Consent to publish This manuscript has been approved by all authors and is solely the work of the authors named.

References

1. Takahashi K, Yamanaka S. Induction of pluripotent stem cells from mouse embryonic and adult fibroblast cultures by defined factors. Cell. 2006;2:663–76.
2. Mora C, Serzanti M, Consiglio A, Memo M, Dell'era P,. Clinical potentials of human pluripotent stem cells. Cell Biol Toxicol. 2017;33:351–60.
3. Pellock JM, Hrachovy R, Shinnar S, Baram TZ, Bettis D, Dlugos DJ, et al. Infantile spasms: a U.S. consensus report. Epilepsia. 2010;51:2175–89.
4. Nakashima M, Kato M, Aoto K, Shiina M, Belal H, Mukaida S, et al. De novo hotspot variants in CYFIP2 cause early-onset epileptic encephalopathy. Ann Neurol. 2018;83:794–806.
5. Konietzny A, Bär J, Mikhaylova M. Dendritic actin cytoskeleton: structure, functions, and regulations. Front Cell Neurosci. 2017;11:1–10.
6. Cory GOC, Ridley AJ. Braking WAVEs. Nature. 2002;418:732–3.
7. Derivery E, Lombard B, Loew D, Gautreau A. The wave complex is intrinsically inactive. Cell Motil Cytoskelet. 2009;66:777–90.
8. Schenck A, Bardoni B, Moro A, Bagni C, Mandel JL. A highly conserved protein family interacting with the fragile X mental retardation protein (FMRP) and displaying selective interactions with FMRP-related proteins FXR1P and FXR2P. Proc Natl Acad Sci USA. 2001;98:8844–9.
9. Begemann A, Sticht H, Begtrup A, Vitobello A, Faivre L, Banka S, et al. New insights into the clinical and molecular spectrum of the novel CYFIP2-related neurodevelopmental disorder and impairment of the WRC-mediated actin dynamics. Genet Med. 2021;23:543–54.
10. Zhang Y, Kang HR, Han K. Differential cell-type-expression of CYFIP1 and CYFIP2 in the adult mouse hippocampus. Anim Cells Syst (Seoul). 2019;23:380–3.
11. Pathania M, Davenport EC, Muir J, Sheehan DF, López-Doménech G, Kittler JT. The autism and schizophrenia associated gene CYFIP1 is critical for the maintenance of dendritic complexity and the stabilization of mature spines. Transl Psychiatry. 2014;4:1–11.
12. Kang M, Zhang Y, Kang HR, Kim S, Yi Y, Lee S, et al. The CYFIP2 p.Arg87Cys causes neurological defects and degradation of CYFIP2 running. Ann Neurol. 2023;93:155–63.
13. Steichen C, Si-Tayeb K, Wulkan F, Crestani T, Rosas G, Dariolli R, et al. Human induced pluripotent stem (hiPS) cells from urine samples: a non-integrative and feeder-free reprogramming strategy. Curr Protoc Hum Genet. 2017;2017:21.7.1-21.7.22.
14. Zhou T, Benda C, Dunzinger S, Huang Y, Ho JC, Yang J, et al. Generation of human induced pluripotent stem cells from urine samples. Nat Protoc. 2012;7:2080–9.
15. Moralli D, Yusuf M, Mandegar MA, Khoja S, Monaco ZL, Volpi EV. An improved technique for chromosomal analysis of human ES and iPS cells. Stem Cell Rev Rep. 2011;7:471–7.
16. Ahn LY, Coatti GC, Liu J, Gumus E, Schaffer AE, Miranda HC. An epilepsy-associated ACTL6B variant captures neuronal hyperexcitability in a human induced pluripotent stem cell model. J Neurosci Res. 2021;99:110–23.
17. Lee Y, Zhang Y, Kang H, Bang G, Kim Y, Kang HR, et al. Epilepsy- and intellectual disability-associated CYFIP2 interacts with both actin regulators and RNA-binding proteins in the neonatal mouse forebrain. Biochem Biophys Res Commun. 2020;529:1–6.
18. Zhang Y, Kang H, Lee Y, Kim Y, Lee B, Kim JY, et al. Smaller body size, early postnatal lethality, and cortical extracellular matrix-related gene expression changes of Cyfip2-null embryonic mice. Front Mol Neurosci. 2019;11:1–5.
19. Lee SH, Zhang Y, Park J, Kim B, Kim Y, Lee SH, et al. Haploinsufficiency of Cyfip2 causes lithium-responsive prefrontal dysfunction. Ann Neurol. 2020;88:526–43.
20. Zhou T, Benda C, Duzinger S, Huang Y, Li X, Li Y, et al. Generation of induced pluripotent stem cells from urine. J Am Soc Nephrol. 2011;22:1221–8.
21. Si-Tayeb K, Idriss S, Champon B, Caillaud A, Pichelin M, Arnaud L, et al. Urine-sample-derived human induced pluripotent stem cells as a model to study PCSK9-mediated autosomal dominant hypercholesterolemia. DMM Dis Models Mech [Internet]. 2016;9:81–90.
22. Bharadwaj S, Liu G, Shi Y, Wu R, Yang B, He T, et al. Multipotential differentiation of human urine-derived stem cells: potential for therapeutic applications in urology. Stem Cells. 2013;31:1840–56.
23. Cheng L, Lei Q, Yin C, Wang HY, Jin K, Xiang M. Generation of urine cell-derived non-integrative human iPSCs and iNSCs: a step-by-step optimized protocol. Front Mol Neurosci. 2017;10:1–8.
24. Wezel F, Pearson J, Kirkwood LA, Southgate J. Differential expression of oct4 variants and pseudogenes in normal urothelium and urothelial cancer. Am J Pathol. 2013;183:1128–36.
25. Atlasi Y, Mowla SJ, Ziaee SAM, Gokhale PJ, Andrews PW. OCT4 spliced variants are differentially expressed in human pluripotent and nonpluripotent cells. Stem Cells. 2008;26:3068–74.

Publisher's Note Springer Nature remains neutral with regard to jurisdictional claims in published maps and institutional affiliations.

Springer Nature or its licensor (e.g. a society or other partner) holds exclusive rights to this article under a publishing agreement with the author(s) or other rightsholder(s); author self-archiving of the accepted manuscript version of this article is solely governed by the terms of such publishing agreement and applicable law.